Environ Earth Sci (2012) 66:889–902
DOI 10.1007/s12665-011-1299-y

ORIGINAL ARTICLE

Delineation of groundwater provenance in a coastal aquifer using statistical and isotopic methods, Southeast Tanzania

Said Suleiman Bakari · Per Aagaard ·
Rolf D. Vogt · Fridtjov Ruden · Ingar Johansen ·
Said Ali Vuai

Received: 26 March 2010 / Accepted: 8 August 2011 / Published online: 3 September 2011

Abstract Rapid population growth and urbanization has placed a high demand on freshwater resources in southeast costal Tanzania. In this paper, we identify the various sources of groundwater and the major factors affecting the groundwater quality by means of multivariate statistical analyses, using chemical tracers and stable isotope signatures. The results from hierarchical cluster analyses show that the groundwater in the study area may be classified into four groups. A factor analysis indicates that groundwater composition is mainly affected by three processes, accounting for 80.6% of the total data variance: seawater intrusion, dilution of groundwater by recharge, and sewage infiltration. The hydrochemical facies of shallow groundwater was mostly of the Na–Ca–Cl type, although other water types were also observed. The deep groundwater samples were slightly to moderately mineralized and they were of the $NaHCO_3$ type. This water type is induced mainly by dissolution of carbonate minerals and modified by ion exchange reactions. The signal from the stable isotope composition of the groundwater samples corresponded well with the major chemical characteristics. In the shallow groundwater, both high-nitrate and high-chloride concentrations were associated with localized stable isotope enrichments which offset the meteoric isotopic signature. This is inferred to be due to the contamination by influx of sewage, as well as intrusion by seawater. The depleted stable isotope values, which coincides with a chemical signature for the deep aquifer indicates that this deep groundwater is derived from infiltration in the recharge zone followed by slow lateral percolation. This study shows that a conceptual hydrogeochemical interpretation of the results from multivariate statistical analysis (using HCA and FA) on water chemistry, including isotopic data, provides a powerful tool for classifying the sources of groundwater and identifying the significant factors governing the groundwater quality. The derived knowledge generated by this study constitutes a conceptual framework for investigating groundwater characteristics. This is a prerequisite for developing a sound management plan, which is a requirement for ensuring a sustainable exploitation of the deep aquifer water resource in the coastal area of Tanzania.

Keywords Groundwater · Multivariate statistical analyses · Stable isotopes · Costal aquifer · Tanzania

Introduction

There is a rapidly increasing demand for freshwater in southeast costal Tanzania due to rapid population growth and urbanization. Until recently, most of the water supply

S. S. Bakari (✉) · P. Aagaard
Department of Geosciences, University of Oslo,
Blindern, P.O. Box 1047, 0316 Oslo, Norway
e-mail: s.s.bakari@geo.uio.no

R. D. Vogt
Department of Chemistry, University of Oslo,
Blindern, P.O. Box 1033, 0316 Oslo, Norway

F. Ruden
Ruden Aquifer Development Ltd, 1628 Engelsviken, Norway

I. Johansen
Department of Environmental Technology,
Institute for Energy Technology, P.O. Box 40,
2027 Kjeller, Norway

S. A. Vuai
Department of Physical Sciences, The University of Dodoma,
P.O. Box 259, Dodoma, Tanzania

has been drawn from the Ruvu River. This is the single most important source of water in the area, involving significant operational costs. Prolonged droughts and deforestation have adversely affected the runoff characteristics within the river basin. Presently, more than 1,800 shallow wells have been drilled to exploit the upper part of the coastal aquifer. The majority of these wells are <100 m deep, with greatly varying capacities and water qualities (JICA 2005). To meet the increasing water demand, the Dar es Salaam Water Supply Authority (DAWASA) has commenced a search for potential groundwater sites in the area. After drilling six deep wells of up to 610 m at Kimbiji, Mpiji, and Mpera, a deep, regional Neogene aquifer was discovered in the alluvial plain in the coastal area of Dar es Salaam (Fig. 1). These findings indicated that this aquifer system was very large and could potentially be a future source of groundwater supply to the public in the region. Especially relevant was the existence of strong artesian conditions in the confined units, with a flowing well discharging more than 3 L s^{-1} (Ruden 2007).

Sustainable management of this resource is dependent on better knowledge of the groundwater system's recharge provenance and hydrogeochemical evolution. It is especially important to understand the processes and factors that control the evolution of saline water in the aquifers. The hydrochemical differentiation of salinization processes in coastal areas is often complex due to the co-existence of other pressures, such as sources of anthropogenic pollution and seawater intrusion (Richter and Kreitler 1993; Morell et al. 1996; Stoessell 1997; Ozler 2003). The study area is a generic example of this challenge, being a coastal area that is experiencing seawater intrusion and which is subjected to multiple anthropogenic pressures, particularly affecting the shallow aquifer.

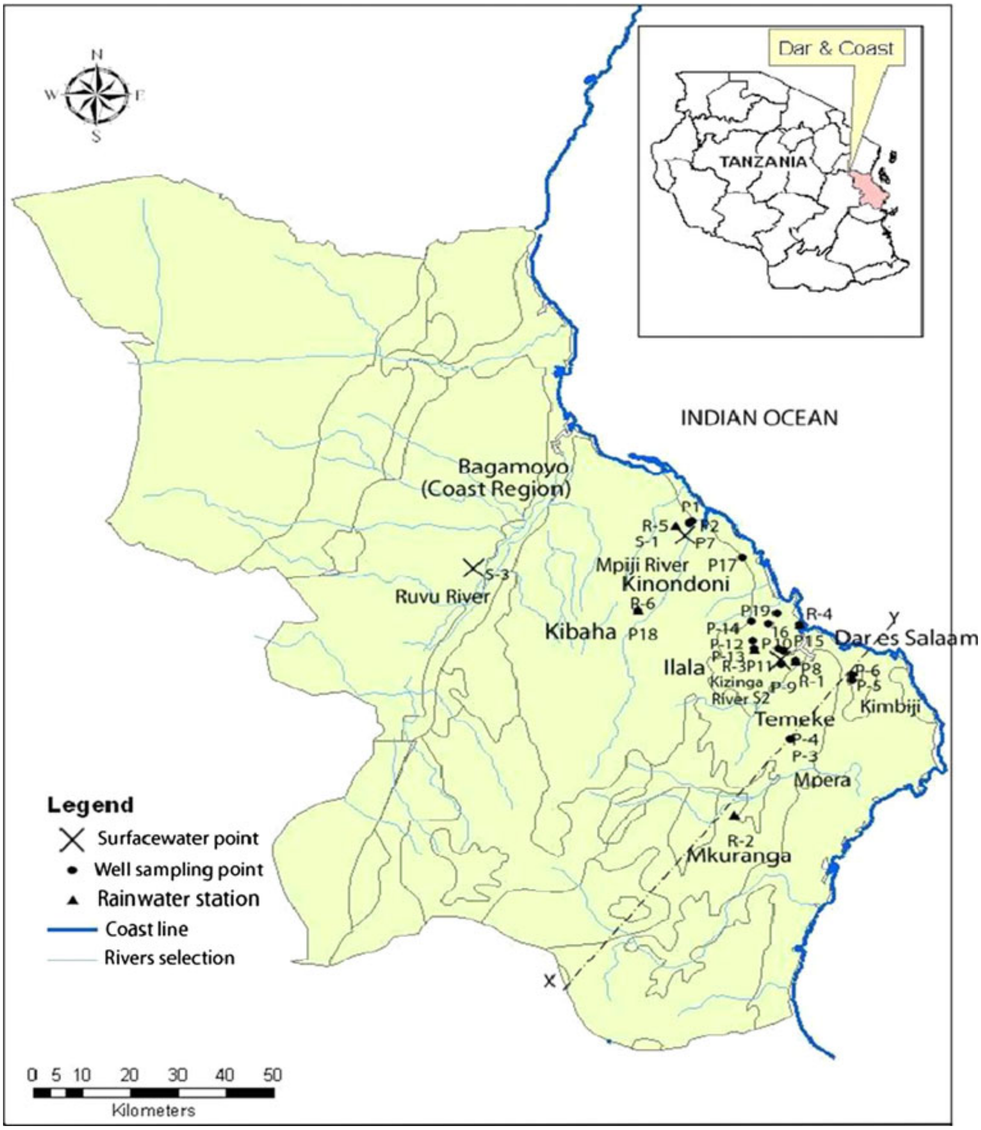

Fig. 1 A map showing the study areas and locations of water sampling points from surface water, rainwater, and groundwater wells. The *designated cross-section line XY* indicates the geological profile of the study area as shown in Fig. 2 below. Map of coastal Tanzania after (Kent et al. 1971)

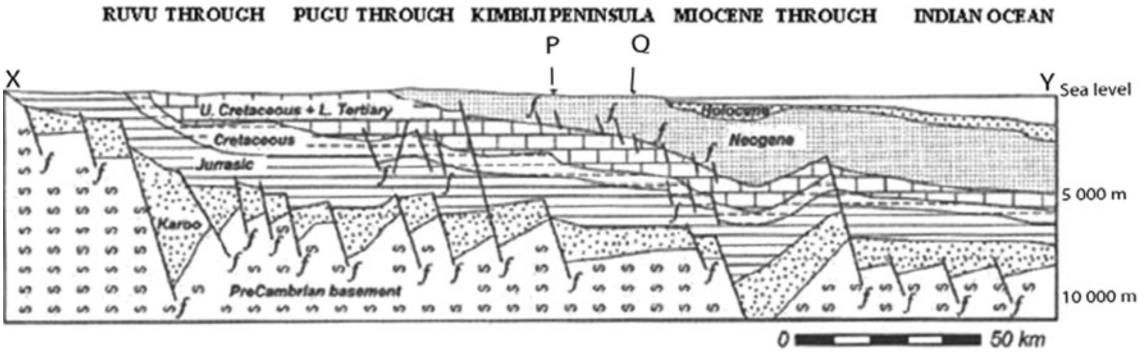

Fig. 2 *Cross-section line XY* as indicated in Fig. 1 above shows the regional geological context of the Kimbiji Neogene Aquifer, Tanzania. ‘P’ and ‘Q’ are designated as the approximate positions for deep wells P-4 (Mpera) and P-6 (Kimbiji), respectively. Profile after TPDC (2007). The aquifer coincides with the Neogene deposits shown on profile

We attempt here to improve our methodology for classifying groundwater samples and identifying significant factors governing water quality. The paper illustrates how one can employ conceptual geochemical reasoning to interpret results from multivariate statistical analysis of data on groundwater chemistry and environmental isotopes. A statistical approach is a powerful tool for identifying the empirical influence of measured variables on the overall physicochemical composition of groundwater. Hierarchical cluster analysis (HCA) and factor analysis (FA) are multivariate statistical methods that are commonly used for the assessment of groundwater quality (Word 1963; Suk and Lee 1999; Helina et al. 2000; Adams et al. 2001; Lee et al. 2001; Thyne et al. 2004; Kim et al. 2005a, b). Stable isotopes of the water molecule (δ^{18}O and δ^{2}H) have been widely and successfully used as inert tracers providing insight into the origin of different water, their recharge processes, residence times in the aquifer and evidence of mixing with connate, thermal or seawater-derived fluids. Such information complements data on the physical hydrology, geophysics, and geochemistry (Kharaka and Carothers 1986; Cook and Herczeg 2000; Kim et al. 2003; Burnett et al. 2006).

This paper focuses on three main objectives: (1) to classify groundwater samples into groups that are governed by the same hydrogeochemical processes using HCA; (2) to identify and describe the main factors affecting groundwater quality in each group, using FA; (3) and to investigate the origin of the recharge and groundwater evolution using chemical species and stable isotope signatures (δ^{18}O, δ^{2}H).

Hydrogeological settings and aquifer characteristics of the study area

The study area comprises the southeastern catchment of the coastal rivers within Dar es Salaam, including the Mpiji, Kizinga and Ruvu rivers (Fig. 1). All rivers and groundwater drain into the Indian Ocean. The area has a tropical climate, with temperatures ranging from 18.1 to 32.2°C and a mean annual temperature of 25.7°C. The mean annual precipitation is 1,124 mm, with a mean yearly potential evapotranspiration of 1,900 mm. The topography of the study area is mostly a low lying terrain, with increasing altitudes from about 20 m a.s.l. around the city center to about 260 m a.s.l. at a distance of about 30 km from the coastline.

The broader geological setting of the study area is described by Kent et al. (1971). The coastal Neogene Aquifer consists of heterogeneous and layered Neogene (Miocene) sands, overlying an assumed geological basement of Lower Tertiary (Eocene) carbonates. From Dar es Salaam and northwards, the Neogene is overlain by thick Holocene deposits, but to the south, Neogene sands are exposed over an area of ~10,000 km^2, between 39°E–39°45′E and 6°30′S–7°30′S, south of Dar es Salaam. The physical boundaries of the Neogene sands have not yet been ascertained, as surveys so far have been restricted to the central areas of the Kimbiji Peninsula, where thicknesses of the Neogene sands are know to exceed 1,000 m (Fig. 2).

The results from pumping tests of two deep wells at Kimbiji indicated the presence of an unconfined aquifer in the upper parts of the wells and a confined aquifer in the lower parts, with strong artesian flow characteristics of more than 3 L s^{-1} (Ruden 2007). Based on a drilling report of six deep wells in the study area (NORCONSULT 2008), borehole cross sections show primarily that alluvium and granular material comprise the upper, unconfined freshwater aquifer. It is also described as consisting of fine to medium sand that contains varying amounts of silt and clay. The unconfined aquifer is shallow in its southwestern part, with an average thickness of 10 m. It is deeper in the eastern part of the study area, up to 50 m. The depth of the water table in the unconfined aquifer ranges from at or near the land surface in low-lying areas to tens of meters below the surface in areas of higher elevation. The upper aquifer is of special significance for the present water supply because most of the groundwater used in Dar-es-Salaam City is withdrawn from this zone (JICA 2005).

The lower confined aquifer is comprised mainly of medium to coarse sands, and sometimes gravels and pebbles occur, interbedded with clayey-rich material. There is no obvious lithological boundary between the two aquifer units, apart from the numerous and nearly cyclic sand and marl beds. Consequently, a gradual transition from upper unconfined to lower confined conditions is expected. A seismic overview study of the area (TPDC 2007) suggests that the average saturated thickness of the aquifer system is around 1,000 m, and the overall flow direction is from west to east, driven by artesian pressure arising from the western hinterland.

There are no prominent agricultural activities in the study area; however, some of the shallow wells are located in the squatter settlements in Dar es Salaam, an area which is characterized by high-population densities and a poor sanitation system.

Materials and methods

Sampling and chemical analysis

Groundwater samples were collected from 13 shallow wells (<100 m) and six deep wells (up to 610 m depth), representing the upper and lower aquifer systems around the coastal watershed, respectively (Fig. 1). Three river water samples in their base flow conditions, six rainwater samples, and one sample of seawater were also collected. The water sampling from wells and streams was conducted between the 17th and 27th of April, 2009. The rainwater samples were collected using a high-density polyethylene funnel (25 cm in diameter), which was connected to a 5 L plastic container, placed 1 m above ground level. The container was covered with aluminium foil to minimize evaporation. The sampling collectors were installed at the end of March, 2009 and collected 1 month later. The seawater sample was collected in January, 2010, at the Slipway shore area in Dar es Salaam.

General procedures for water sampling, preservation, transportation, and chemical analyses were conducted according to ISO standard (IMPACTS manuals) (Vogt et al. 2001). Sampling from the deep and shallow wells was performed using a bailer sampler and water pumps, respectively, except for the well with artesian flow conditions. The samples were collected in 250-mL high-density polyethylene (HDPE) bottles, after passing through 0.45 μm syringe filters. Prior to filtration, temperature, electrical conductivity (EC), pH, oxidation–reduction potential (ORP), and dissolved oxygen (DO) were measured using portable meters (Hach USA). Total alkalinity was measured by potentiometric titration with 0.1600 N H_2SO_4 to a pH end point of 4.5 (Hach 1992) on the same day of sampling at Ardhi University in Dar es Salaam. All other chemical analyses were performed at the University of Oslo, Norway, within a month from sampling. Dissolved concentrations of anions Cl^-, Br^-, NO_3^- and SO_4^{2-} and the major cations Ca^{2+}, Mg^{2+}, K^+ and Na^+ were analyzed by means of Dionex ion chromatography (IC) using ICS-1000 and ICS-2000 columns for the anions and cations, respectively. The overall charge discrepancy between cations and anions was less than ±5%, except for one rainwater sample (R-1), which had a 20% cation deficiency. Concentrations of Mn were measured with Perkin–Elmer, Inductively Coupled Plasma-Mass Spectrometry (Norwalk, CT, USA). The instrument was calibrated to the multi-element standard. The relative standard deviation for replicates of all the Mn analyses was within ±5%.

Stable isotopes analyses

Unfiltered samples for stable isotope analyses were collected in 50-mL HDPE bottles and sealed with PE caps. The samples were stored at 4°C in the laboratory prior to analysis. The isotopic measurements were conducted at the Institute for Energy Technology in Kjeller, Norway. The concentrations are given in δ-units, calculated with respect to Vienna Standard Mean Ocean Water (VSMOW) according to Eq. 1.

$$\delta_{\text{sample}}(‰) = 1{,}000\left[\frac{R_{\text{sample}} - R_{\text{VSMOW}}}{R_{\text{VSMOW}}}\right] \quad (1)$$

where, R_{sample} and R_{VSMOW} are the isotopic ratios of the sample and VSMOW, respectively. Samples were measured at least in duplicates, providing a measure for precision of the analytical measures of ±0.1‰ for $\delta^{18}O$ and ±1‰ for $\delta^{2}H$. International Atomic Energy Agency (IAEA) reference materials were used throughout the isotopic water analyses to ensure a high quality of the data.

Multivariate statistical analysis

Data on 13 physicochemical variables, i.e., DO, pH, EC, Ca^{2+}, Mg^{2+}, Na^+, K^+, HCO_3^-, Cl^-, Br^-, SO_4^{2-}, NO_3^- and Mn^{2+}, for the 28 water samples were assessed using multivariate statistical techniques. The data (Table 1) were normalized to give each variable equal weight in the multivariate statistical analysis and thereby to prevent results from being influenced most strongly by the variable with the greatest absolute magnitude and span (Thyne et al. 2004).

Hierarchical cluster analysis (HCA) and factor analysis (FA) were used for the multivariate analysis. The HCA method is used to produce a graphical representation of

Table 1 Results of water samples analyses in the study area

Sample code	Village	Depth (m)	pH	Temp. (°C)	DO (mg L^{-1})	ORP (mV)	EC (μs/cm)	Na^+ (mmole L^{-1})	K^+ (mmole L^{-1})	Mg^{2+} (mmole L^{-1})	Ca^{2+} (mmole L^{-1})	Cl^- (mmole L^{-1})	NO_3^- (mmole L^{-1})	SO_4^{2-} (mmole L^{-1})	HCO_3^- (mmole L^{-1})	Br^- (μmole)	Mn^{2+} (μmole)	δ^2H (‰)	$\delta^{18}O$ (‰)	Saturation indices (SI)		
																				Calcite	Dolomite	Gypsum
Deep groundwater samples																						
P-1	Mpiji	200	7.71	30.2	2.13	nm	1,057	8.199	0.014	0.504	0.502	4.183	0.055	0.360	4.294	32.66	3.1952	−15.2	−4.05	0.08	0.35	−2.62
P-2	Mpiji	610	7.76	29.7	2.46	nm	2,570	19.73	0.150	0.676	1.674	19.65	0.193	0.691	3.016	38.45	0.4118	−9.10	−4.05	0.39	0.57	−1.99
P-3	Mpera	200	6.16	28.5	1.89	nm	362	1.957	0.084	0.139	0.245	1.366	0.036	0.208	0.803	29.84	0.9110	−13.6	−4.84	−2.40	−4.86	−2.97
P-4	Mpera	600	6.35	30.8	2.48	nm	359	2.371	0.082	0.181	0.132	1.384	0.035	0.133	1.115	30.22	1.3210	−14.0	−4.81	−8.05	−15.8	−9.18
P-5	Kimbiji	200	7.85	30.1	1.39	−51.1	1,154	9.308	0.373	0.098	0.409	4.077	0.040	0.345	5.917	31.34	0.3412	−13.7	−5.11	0.25	0.07	−2.73
P-6	Kimbiji	612	8.33	34.6	0.49	−81.2	866	8.264	0.112	0.015	0.065	2.035	0.037	0.185	5.720	30.01	0.3666	−13.5	−4.77	−0.03	−0.47	−3.76
Shallow groundwater samples																						
P-7	Mpiji	80	7.79	29.6	6.35	nm	848	2.480	0.079	0.387	1.173	2.738	0.000	0.137	2.614	30.77	2.4291	−11.1	−3.97	0.35	0.40	−2.61
P-8	Kijichi	50	6.88	29.3	5.44	nm	358	2.212	0.117	0.035	0.609	0.927	0.327	0.162	1.770	29.56	0.2993	−14.6	−4.79	−0.97	−3.00	−2.73
P-9	Mbagala	70	6.32	28.1	4.84	nm	1,050	7.960	0.220	0.694	0.624	5.835	2.455	0.723	1.016	34.42	0.7497	−12.7	−4.89	−1.90	−3.58	−2.28
P-10	Tandika	53	5.80	28.5	3.5	88.7	1,197	5.497	0.975	1.546	1.880	4.097	7.176	0.825	0.344	30.65	3.8939	−9.50	−4.43	−2.46	−4.84	−1.88
P-11	Tazara	65	6.76	28	6.64	28.2	860	4.131	0.695	1.230	0.913	3.122	2.961	0.650	1.492	30.47	2.2904	−10.0	−4.65	−1.13	−1.96	−2.18
P-12	Tabata	60	6.87	28.9	6.56	25.2	1,211	11.73	0.150	0.527	0.160	9.959	0.048	0.379	1.885	37.06	0.7901	−11.7	−5.70	−1.64	−2.58	−3.10
P-13	Airport	100	7.53	28.7	4.01	−16.6	1,168	10.44	0.169	0.411	0.155	5.397	0.036	0.419	4.376	33.01	0.3852	−12.6	−6.07	−0.63	−0.66	−3.07
P-14	Kigogo	60	7.17	29.5	4.46	42	3,870	19.43	0.169	1.691	7.902	28.25	1.019	2.217	4.737	54.05	7.0770	−14.3	−5.73	0.56	0.64	−1.04
P-15	Ocean road	11	7.43	28.4	4.4	−11	1,097	3.045	0.453	0.103	2.733	2.894	0.891	0.509	4.327	32.18	0.0608	−11.7	−3.39	0.49	−0.27	−1.80
P-16	M'nyamala	50	7.08	28	3.69	9.5	1,696	7.395	1.662	0.236	3.017	6.879	2.804	0.786	3.491	32.76	3.3639	−11.4	−2.70	0.03	−0.88	−1.66
P-17	Tegeta	65	6.92	28.6	4.46	19.1	6,130	29.18	0.271	3.164	14.01	40.04	0.942	9.666	3.508	65.64	0.1455	−10.4	−2.19	0.29	0.11	−0.34
P-18	Kibaha	95	7.31	27.3	2.01	−4.3	5,100	30.88	0.183	4.808	3.844	38.03	0.000	4.399	5.556	40.36	0.1637	−8.10	−1.79	0.39	1.03	−1.11
P-19	Ubungo	70	6.23	26.8	6.13	59.9	1,790	12.37	0.100	1.794	0.898	13.76	0.238	0.558	1.115	43.28	2.5674	−12.8	−3.38	−1.82	−3.20	−2.30
SW	Slipway		7.43	28.7	nm	nm	49,000	408.9	7.42	48.54	9.46	507.04	0.29	26.44	2.96	838.51	nm	nm	nm	0.26	1.44	−0.68
Surface water samples																						
S-01	Mpiji		7.82	28.4	5.8	nm	688	0.261	0.113	0.024	1.043	0.105	0.039	0.033	2.065	5.16	1.4082	−12.9	−2.92	0.27	−0.93	−3.17
S-02	Kizinga		7.38	27.6	5.65	nm	651	3.480	0.187	0.481	0.609	3.436	0.253	0.231	1.328	6.07	0.9712	−7.00	−1.66	−0.65	−1.25	−2.65
S-03	Ruvu		7.8	26.5	7.09	−33.3	97.4	0.217	0.041	0.156	0.177	0.092	0.138	0.093	0.574	28.08	0.3665	−9.50	−2.77	−1.05	−2.00	−3.39
Rainwater samples																						
R-1	Kijichi		6.23	26.9	7.75	nm	24.2	0.015	0.002	0.004	0.018	0.019	0.004	0.004	0.064	30.57	0.0003	−23.2	−4.61			
R-2	Mkuranga		5.93	26.2	7.69	nm	26.4	0.139	0.012	0.018	0.021	0.150	0.007	0.011	0.061	2.82	0.0004	−18.1	−3.73			
R-3	Airport		6.08	28.2	6.52	nm	18.24	0.092	0.018	0.011	0.033	0.095	0.003	0.012	0.086	30.09	0.0006	−6.60	−2.24			
R-4	Ocean road		6.95	25.6	7.12	nm	65.3	0.086	0.019	0.014	0.233	0.099	0.035	0.024	0.363	2.81	0.0042	−24.2	−4.99			
R-5	Bagamoyo		6.02	24.1	8.25	nm	19.33	0.037	0.011	0.008	0.050	0.044	0.006	0.007	0.100	0.00	0.0009	−5.50	−2.04			
R-6	Kibaha		6.07	26.1	8.06	nm	42.6	0.040	0.009	0.010	0.155	0.047	0.005	0.012	0.307	28.27	0.0028	−3.60	−2.54			

nm not measured, *SW* seawater

sample groups using dendrograms. As such, this method is well suited to identify hydrochemical facies. An agglomerative hierarchical clustering was applied, using a combination of the Word's linkage method (Word 1963; Suk and Lee 1999), where squared Euclidean distances was used as a measure of similarity between every pair of objects (Thyne et al. 2004; Kim et al. 2005a, b).

The FA explains relationships between measured variables and thus may be used to infer the hydrogeochemical processes that control water chemistry (Suk and Lee 1999; Helina et al. 2000; Kim et al. 2005a). The FA takes the data organized in a correlation matrix and rearranges them in a manner that better explains the structure of the underlying system that produced the data. Therefore, the matrix of correlation coefficients measures how well the variance of each constituent can be explained by its relationships with each of the others. The statistical analytical procedures were conducted using the statistical software package MINITAB (version 15, Minitab Inc., USA).

Results and discussion

Physicochemical data

The physicochemical and stable isotopic compositions of the water samples are summarized in Table 1. Electrical conductivity (EC) of groundwater varied widely, from 358 to 6,130 μS cm^{-1}. The highest EC value was observed in a shallow groundwater sample <5 km from the coast, indicating the presence of saline groundwater intrusion. Oxidation–reduction potential (ORP) fluctuated from reducing (−81.2) to oxidative (88.7 mV) conditions and both ORP and dissolved oxygen concentration (DO) decreased exponentially with depth. The anoxic conditions in the deep aquifer may be due to the mineralization of organic matter. This may have occurred either upon passing through organic-rich surface layers in the recharge zone or by oxidation of dissolved organic matter brought down with the percolating soil water. Groundwater was slightly acidic to alkaline, with pH ranging from 5.80 to 8.33. Concentrations of HCO_3^- were the highest in the deep groundwater, reaching up to 361 mg L^{-1}. Weathering of Eocene carbonate rocks comprising the basement of the aquifer system is believed to be the main source for the high-bicarbonate concentrations in the deep groundwater. Saturation indices (SI) for selected minerals, calculated by the hydrogeochemical code PHREEQC (Parkhurst and Appelo 1999) using the chemical data, show that most of the deep groundwater samples are supersaturated with respect to calcite and dolomite (Table 1). This suggests that it is these carbonate minerals that are governing the bicarbonate concentrations in the deep aquifers.

Multivariate analysis and groundwater quality

Hierarchical cluster analysis

Hierarchical cluster analysis (HCA) was performed to sort the samples into a finite number of groups with similar hydrochemical compositions, and therefore inferred similar processes governing their physiochemistry. Figure 3 shows the resulting dendrogram classifying the samples into four groups (A, B, C, D). The affiliation of the sample groups are easily recognized on the basis of the varying salinity contents for the groups A, C and D, and nitrate concentrations for group B. Group A represents the groundwater with high HCO_3^- concentrations and moderate salinity. More than half of the groundwater samples in group A are from the deep aquifer with strongly reducing conditions. Group B had significantly higher nitrate and potassium concentrations (Table 1; Fig. 3) than those of the other groups, indicating that this group has been severely contaminated. These high-nutrient values are most likely due to leakage from domestic wastewater, since these samples are all from wells situated in the squatter settlements of Dar es Salaam. This area is characterized by a high-population density and poor sanitation infrastructure. Group C comprises the samples with low and intermediate salinity. This group comprises all surface and rainwater samples in addition to some groundwater samples. Group D contains the most saline groundwater samples with high-EC and some Cl^- content. This is most likely due to seawater intrusion into the coastal area.

Factor analysis

Table 2 gives the parameter loading of the first three extracted factors, which together explained 80.6% of the total data variance in the dataset. The varimax-rotated factor loadings and factor scores for the first two factors are presented in Fig. 4. Factor I, explaining 44.5% of the total data variance, presents significant and positive loading with EC, Na^+, Cl^- and Br^-, as well as with Ca^{2+}, Mg^{2+} and SO_4^{2-}. Factor I is, therefore, conceptually interpreted to express the degree of salinization and thereby saltwater intrusion. Water samples in group D of the cluster analysis, therefore, have strong positive scores, while samples in group C have negative scores along this factor (Fig. 4b). High-ionic strength may in some cases simply be due to up-concentration by evaporation (Liu et al. 2003; Ceron et al. 2000), although in this case seawater intrusion appears to be the main governing process. Salinization by mixing with seawater is also confirmed by the Na^+/Cl^- and Br^-/Cl^- ratios (Fig. 7), as well as the $\delta^{18}O$–Cl^- relationship (Fig. 8).

Factor II, explaining an additional 19.1% of the total variance (Table 2), possesses strong negative loadings of HCO_3^- and pH, and a high-positive loading of dissolved

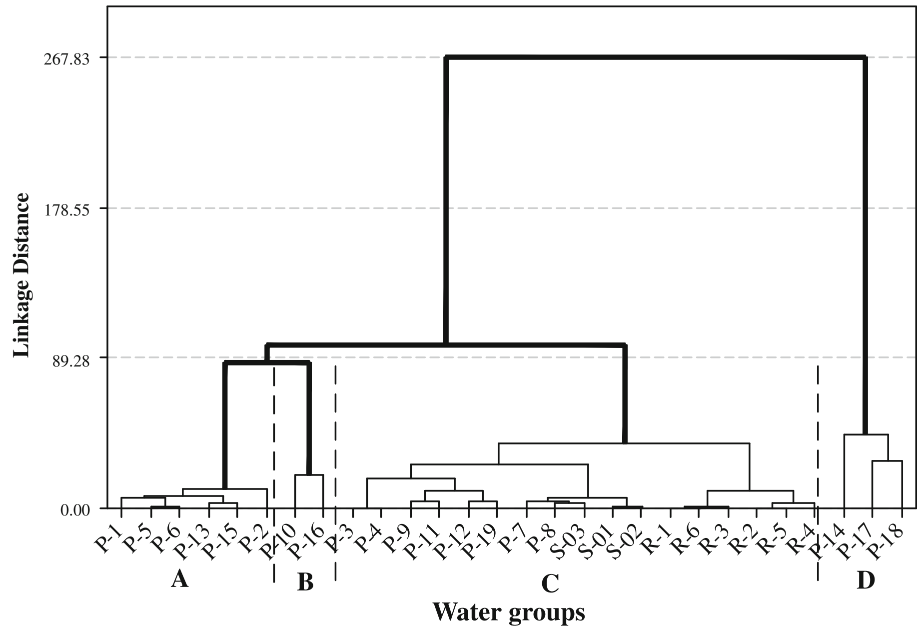

Fig. 3 Dendrogram (samples) from hierarchical cluster analysis using Ward's method as a linkage rule, and the squared Euclidian distance as a measure of similarity

Table 2 Rotated factor loading of three factors after varimax rotation, significant loading were shown as bold fonts

Variable	Factor I	Factor II	Factor III
pH	0.00	**−0.87**	−0.17
DO	−0.19	**0.77**	−0.24
EC	**0.96**	−0.25	0.10
Na^+	**0.90**	−0.35	0.03
K^+	0.04	−0.10	**0.86**
Mg^{2+}	**0.88**	−0.03	0.12
Ca^{2+}	**0.88**	−0.04	0.16
Mn^{2+}	0.15	−0.14	**0.69**
Cl^-	**0.97**	−0.17	0.01
NO_3^-	0.07	0.21	**0.90**
SO_4^{2-}	**0.94**	−0.00	−0.01
HCO_3^-	0.36	**−0.89**	0.05
Br^-	**0.71**	−0.25	0.22
Eigenvalues	5.779	2.489	2.214
% of variances	0.445	0.191	0.170
Cumulative %	44.50	63.60	80.60

oxygen (DO). This factor is descriptive of the process governing the chemistry of the samples in group A in the cluster analysis (see Figs. 3, 4). The opposite strong loading of pH and HCO_3^- to DO translates conceptually into a gradient of the residence time of groundwater. Fresh groundwater contains dissolved organic matter which, over time, becomes mineralized, thus reducing the DO. This generates CO_2, which in water forms carbonic acid that dissociates to H^+ and HCO_3^- ions. The acidity that is generated is consumed by enhanced weathering of calcite and carbonate rocks in the aquifer basement, resulting in increased concentrations of pH and HCO_3^-. A confounding issue along this factor is the high-positive scores of samples that are contaminated by sewage (group B in

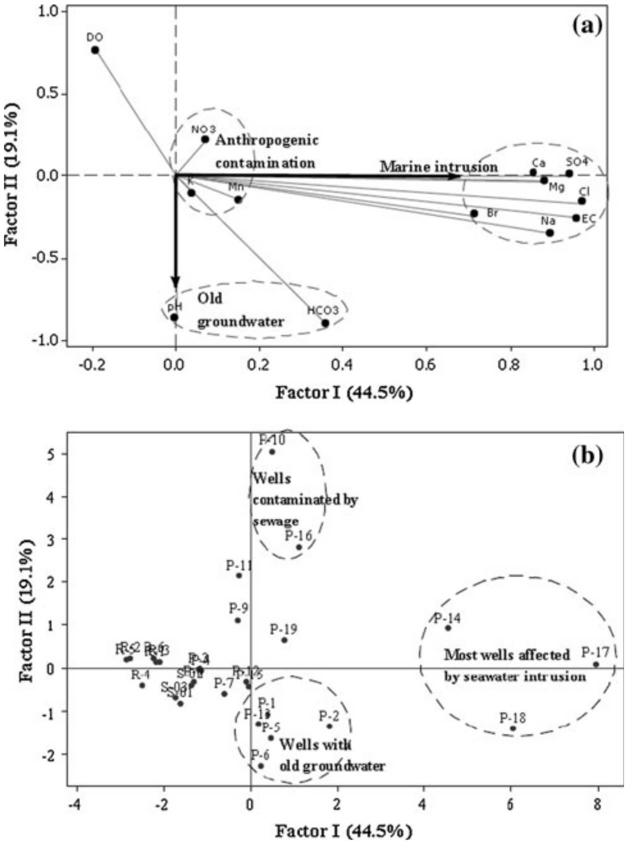

Fig. 4 Varimax-rotated factor loadings (**a**) and factor scores (**b**) for the first two factors of hydrochemical parameters of the groundwater in the study area

Table 3 Pearson correlation coefficients for 13 hydrogeochemical variables of water samples

	pH	DO	EC	Na^+	K^+	Mg^{2+}	Ca^{2+}	Mn^{2+}	Cl^-	NO_3^-	SO_4^{2-}	HCO_3^-	Br^-
pH	1.00												
DO	−0.44	1.00											
EC	0.22	−0.38	1.00										
Na^+	0.26	−0.47	**0.96**	1.00									
K^+	−0.02	−0.23	0.17	0.10	1.00								
Mg^{2+}	0.00	−0.25	**0.87**	**0.85**	0.12	1.00							
Ca^{2+}	0.09	−0.16	**0.87**	**0.71**	0.20	0.65	1.00						
Mn^{2+}	0.04	−0.18	0.25	0.18	0.39	0.20	0.29	1.00					
Cl^-	0.15	−0.31	**0.98**	**0.96**	0.06	**0.88**	**0.82**	0.22	1.00				
NO_3^-	−0.30	−0.11	0.10	0.03	**0.73**	0.21	0.17	0.46	0.02	1.00			
SO_4^{2-}	0.05	−0.20	**0.89**	**0.79**	0.10	**0.78**	**0.92**	0.02	**0.86**	0.09	1.00		
HCO_3^-	**0.74**	**−0.71**	0.57	0.62	0.18	0.35	0.37	0.20	0.49	−0.12	0.34	1.00	
Br^-	0.11	−0.40	**0.71**	**0.71**	0.17	0.56	0.65	0.33	**0.70**	0.16	0.62	0.46	1.00

Coefficients are significant at the 0.05 level and those higher than 0.70 were shown as bold fonts

Fig. 3). Still, these samples constitute relatively young water and as such comply with the overall interpretation.

The third factor, accounting for 17.0% of the total variance, is mainly associated with a high-positive loading for NO_3^- and K^+, and moderate loadings for Mn^{2+}. This factor is, therefore, representative of the factors governing the water chemistry in samples of group B in the cluster analysis. The lower limit of nitrate concentration for Group B samples is 173.9 mg L^{-1}, which is higher than the limit set for drinking water, which is 50 mg L^{-1} as established by WHO Guidelines for drinking-water quality (2004), or 100 mg L^{-1} as established by Tanzania Standard for Rural Water Supplies, Ministry of Water (2006). Both nitrate and potassium are nutrients that are usually kept at low concentrations in nature due to rapid plant uptake. Furthermore, the NO_3^- has no known lithological source and hence it reveals an anthropogenic loading, which is here attributed to wastewater leakage from domestic activities. In addition, K^+ is positively correlated with NO_3^- ($R = 0.73$, see Table 3). This co-variation is likely due to the fact that they are both found in high concentrations in sewage and released by bacterial action during the decomposition of organic material (Appelo and Postman 2005). Furthermore, since neither is correlated with any other major anions and cations (Table 3), it seems likely that they come from the same anthropogenic sources.

Geochemical indicators of origin and groundwater evolution

Stable isotopes and groundwater provenance

Stable δ^2H and $\delta^{18}O$ isotopes are ideal tracers for assessing the recharge areas and flow path of groundwater because they make up the water molecules and they are sensitive to physical processes such as mixing and evaporation/salinization processes (Faure and Mensing 2005). The results of $\delta^{18}O$ and δ^2H analyses are presented in Table 1 and are shown in Fig. 5. Stable isotope values of rainwater are slightly variable from −5.0 to −2.0‰ for $\delta^{18}O$ and from −24.2 to −3.6‰ for δ^2H. The rainwater samples are found to the left of the global meteoric water line (GMWL) of Craig (1961). This is a typical characteristic for tropical climate stations (Dansgaard 1964). The slope of the fitting line for the rainwater data (Fig. 5), given as $\delta^2H = 10.5 + 7.2\delta^{18}O$ ($R^2 = 0.97$), is in agreement with the slope for the

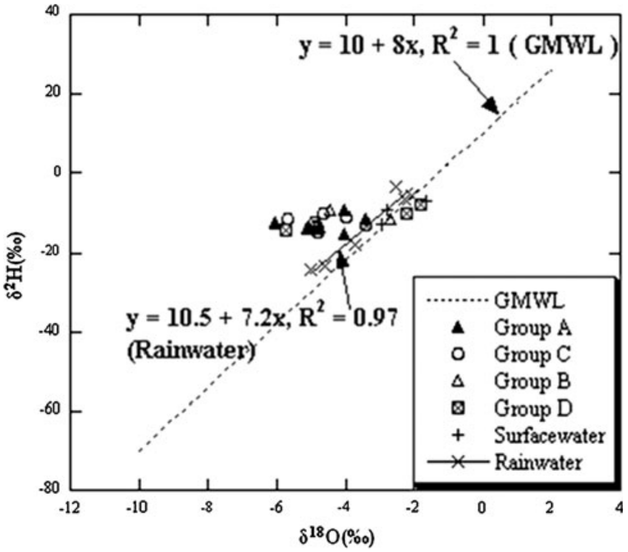

Fig. 5 Stable isotopes plot of the rainwater, surface water and groundwater in the coastal area of Tanzania. Groundwater samples are sorted according to clustered groups

mean monthly isotopic composition reported by Dansgaard (1964) for Dar es Salaam rainwater station ($\delta^2H = 13 + (8 \pm 2)\delta^{18}O$), but is slightly lower than global meteoric water lines ($\delta^2H = 10 + 8\delta^{18}O$, $R^2 = 1$). Such a low slope is common for East African Equatorial sites, where precipitation events are related to air masses with different source characteristics during different seasons and local factors affecting the climate (Nicholson 1996; Rietti-Shati et al. 2000). Stable isotope values of river water are the least negative (between −2.9 and −1.7‰ for $\delta^{18}O$, between −12.9 and −7.0‰ for δ^2H). River water samples from Ruvu and Mpiji rivers are plotted along the same slope as the fitting line of rainwater data and GMWL (Fig. 5), respectively, indicating a predominantly meteoric water source. The Kizinga River sample is the most enriched in $\delta^{18}O$ and plotted below the GMWL (Fig. 5), reflecting a significant effect of evaporation (Clark and Fritz 1997). It appears, therefore, that river water in the study area is mainly supplied by local rainfall. The shallow groundwater in groups B, C, and D had a wide range of stable isotope values ranging from −5.7 to −1.8‰ and −8.1 to −14.3‰ for $\delta^{18}O$ and δ^2H, respectively. This could result from heterogeneity of the recharge conditions due to different flow paths. All groundwater samples show minimal effects from evaporation, except for two of three samples in group D (P-17, P-18) which show significant evaporation and they are plotted below the GMWL. That the observed isotopic values (δ^2H and $\delta^{18}O$) of both shallow and deep groundwater samples are equal to or more depleted than the local precipitation implies that groundwater recharge is accompanied by minimal evaporation (Nkotagu 1996). Stable isotopes of some of the shallow groundwater samples are plotted on the same slope as river water and rainwater (Fig. 5). This may be the result of surface water–ground water interaction or direct infiltration by local precipitation. It appears, therefore, that the shallow groundwater in the coastal aquifer is mainly recharged by modern precipitation and surface water.

In contrast, the groundwater samples in group A show a depleted stable isotope values, which are plotted above the fitting line of the rainwater data and GMWL (Fig. 5). The $\delta^{18}O$ values ranged from −6.1 to −4.0‰, and coincide with the other chemical factors such as DO, pH and HCO_3^- in the study area. This indicates that the deep aquifer is an older groundwater system that is initially fed by shallow groundwater and precipitation. The anoxic conditions in the deep aquifer (Table 1) imply a long residence time. A separate study on age estimation, based on radiocarbon dating in the same study area, suggests that the residence time of deep groundwater is on the order of several thousands of years and reflects past recharge during a colder climate than at present (Bakari et al. in progress).

The origin of groundwater salinity

The multivariate analysis (Figs. 3, 4) shows that groundwater samples in the coastal area are distinctively grouped in terms of salt contents and degree of nitrate contamination. Using ionic ratios and concentrations of major dissolved constituents, the clustered sample groups are clearly distinguished by water types in a Piper diagram (Fig. 6). Group A consists of $NaHCO_3$ type water and represents old groundwater. Group B is more a Na(Mg, Ca)–NO_3 type of water which has been contaminated by sewage. Group D, which is a Na(Mg, Ca)–Cl type of water, represents a more simple freshwater–seawater mixing. This wide range of hydrochemical facies reflects the complexity of the hydrogeochemistry in the study area. It seems that the observed facies for group D (P-14, P-17, P-18), with chloride (Cl^-) as the dominant anion, are the samples that are most influenced by seawater intrusion (Fig. 4b), judging from the elevated EC, Cl^- and high content of Na^+ relative to Ca^{2+}, Mg^{2+} and K^+ (Table 1). The chloride concentration of groundwater samples for group D ranges from 1,003 to 1,422 mg L^{-1}. The variations in concentration of other elements are more difficult to link to this process because their amounts are strongly governed by interactions with aquifer materials such as clay, silt, and sands (Stoessell 1997). In contrast, group C is characterized by low and intermediate salinity water, which includes also rainwater and surface water samples. The hydrochemical facies of the groundwater samples in group C are partially related to surface and rainwater chemical signatures, although their chemistry has been modified by spatially varying conditions. These features are indicative of shallow groundwater that are still in on early evolutionary stage.

If the chemical composition of groundwater samples were only controlled by a simple mixing process with seawater, then the samples would be plotted along the straight dashed line in Fig. 6, connecting the background freshwater and the seawater on the diamond-shape field of the Piper diagram. However, the chemical compositions of coastal groundwater affected by seawater intrusion are also controlled by cation exchange reactions (Appelo 1996). Therefore, the spatial trend in groundwater within the study area primarily shows a curved path (full line) of hydrogeochemical evolution, which starts from the Ca–$NaHCO_3$–Cl type, progresses through the Na–Ca–Cl type, and ends up as the NaCl type of groundwater. This is a typical pattern indicating the cation exchange reaction when seawater intrusion has occurred (Appelo and Postma 1993). Another ion exchange process, found as a gradient in group A samples, is of increasing HCO_3^- concentrations with essentially decreasing Ca^{2+} concentrations, shifting from a more $CaHCO_3$ to a $NaHCO_3$ type of water (plotted in the lower-right portion of the diamond-shape field).

Fig. 6 Piper diagram of water samples in the study area. Samples are sorted according to clustered groups

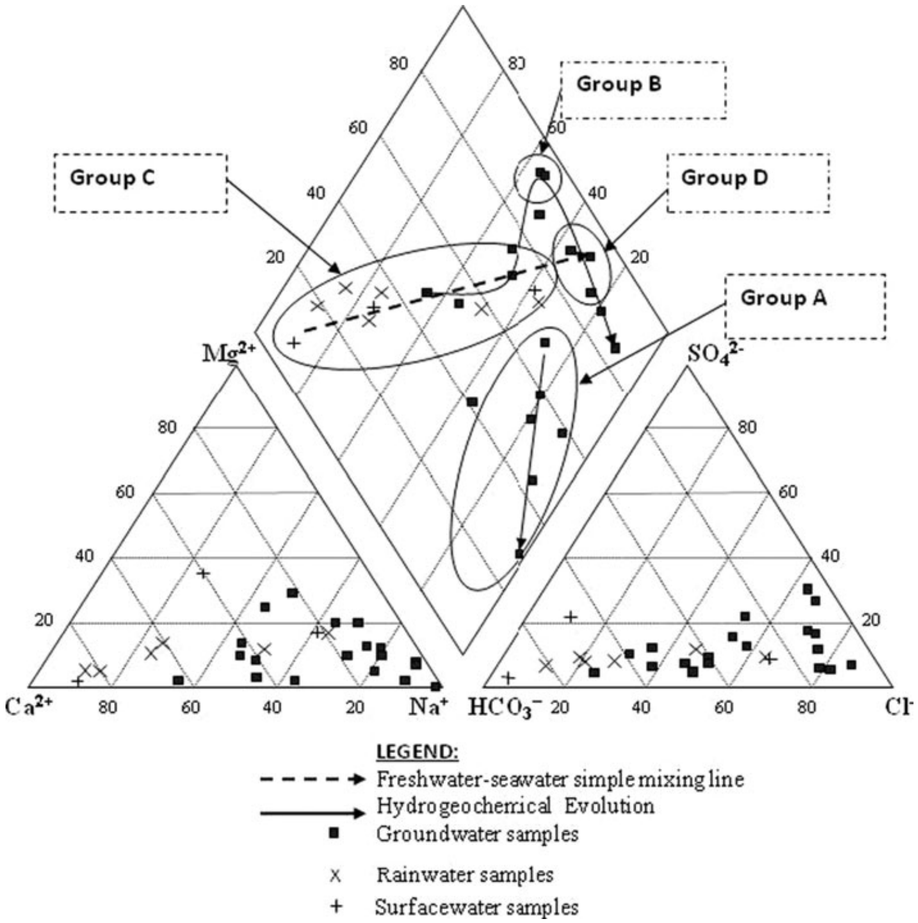

A $NaHCO_3$ water type is referred to as reflecting exchange water since there is more HCO_3^- than alkaline-earth cations (Ca^{2+} and Mg^{2+}) on an equivalent basis (Tijani 2004). These distribution patterns therefore indicate that the groundwater chemistry in the study area is influenced by cation exchange reactions as well as the simple mixing with seawater as a result of seawater intrusion. This concept is also supported by the ionic ratios of both Na^+/Cl^- and Br^-/Cl^- (Fig. 7). Since Na^+ is exchanged for Ca^{2+} and Mg^{2+}, the Na^+/Cl^- ratio, plotted against Cl^- (Fig. 7a) is a good indicator of cation exchange-related changes in the groundwater chemistry (Stigter et al. 2006). Where the degree of groundwater salinization by seawater intrusion increases, the chloride concentration increases accordingly, but the Br^-/Cl^- ratio decreases. The Br^-/Cl^- ratio as a function of the chloride concentration (Fig. 7c) may therefore be used to identify the degree of seawater intrusion in coastal regions (Andreasen and Fleck 1997; Richter and Kreitler 1993). The most saline groundwater samples (group D) have Na^+/Cl^- and Br^-/Cl^- ratios close to that of seawater. Corroborating the findings above, we see that group D comprises the most salinized groundwater samples, with Br^-/Cl^- ratios similar to the seawater ratio (0.0016). The exchange process also affects the concentration of Ca^{2+} relative to bicarbonate (Fig. 7b). In general, the groundwater samples of group A show an increase in the Na^+/Cl^- ratio (Fig. 7a) and a decrease in the Ca^{2+}/HCO_3^- ratio (Fig. 7b) with decreasing Cl^- concentrations. The deep aquifer water samples in group A are, as expected, less salinized and show relatively lower chloride concentrations and higher Br^-/Cl^- ratios. An interesting exception is the deep groundwater sample (P-2), which shows a comparatively high-chloride concentration and low Br^-/Cl^- ratio. One may therefore speculate that this anomaly is linked to relict seawater in this lower aquifer system. During the Pleistocene the sea level stood much higher than today (Johnston 1983), causing the aquifer system to be invaded by seawater to a greater extent. When the sea level dropped to its present position, some of this relict seawater may have remained in the aquifer and showed up in the well producing sample P-2.

Intrusion of marine water into the shallow aquifer has also been reported previously from the Kigamboni Peninsula along the Dar es Salaam coastal strip (Nkotagu 1989). In addition, a few of the boreholes from the Mtwara coastal region of Tanzania were reported to have a mixture of freshwater and seawater (Gondwe 1991).

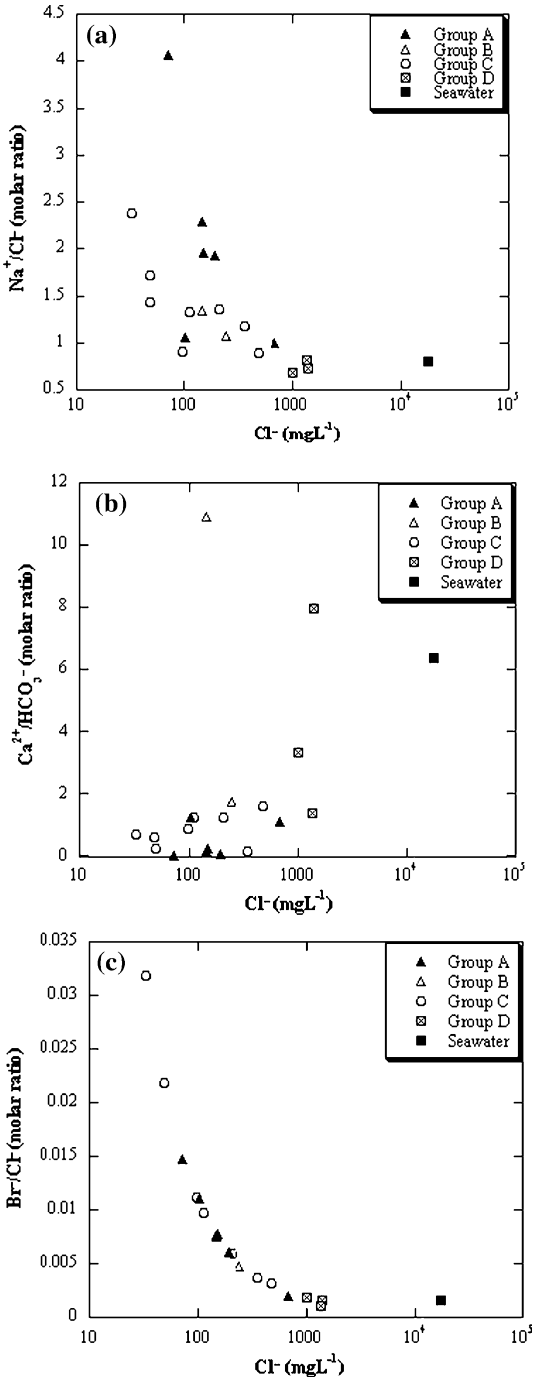

Fig. 7 Relationship between Na^+/Cl^- ratio versus Cl^- (**a**), Ca^{2+}/HCO_3^- ratio versus Cl^- (**b**) and Br^-/Cl^- ratio versus Cl^- concentrations in groundwater samples in the study area. Samples are sorted according to clustered groups

The isotopic variations of oxygen along with other chemical characteristics, such as Cl^- and NO_3^-, are assessed to provide supplementary information on the salinitization process of groundwater in the coastal aquifer. As discussed earlier, the variations in the $\delta^{18}O$ and δ^2H values in fresh water are naturally determined by the recharge regimes. In saline and contaminated groundwater, however, the variations in $\delta^{18}O$ and δ^2H values are also controlled by the composition of the saline and/or contaminant sources. In the shallow groundwater samples of groups B and D, we have observed an increase in $\delta^{18}O$ values with chloride content (Fig. 8a), thus reflecting the enriched $\delta^{18}O$ characteristics of the saline sources. Our data show that the most affected saline groundwater in group D has both high-$\delta^{18}O$ and Cl^- concentrations (Fig. 8a). Given these combined geochemical and isotopic signals, these groundwater samples P-14, P-17 and P-18, classified as group D from the cluster analysis, are interpreted to be derived from a saline source with chemical characteristics that mimic those of sea water intrusion. In contrast, the saline samples from group B (P-10, P-16) have both high-chloride and high-nitrate concentrations (Table 1), although the isotopic variations of $\delta^{18}O$ did not show a clear trend with respect to the nitrate concentrations

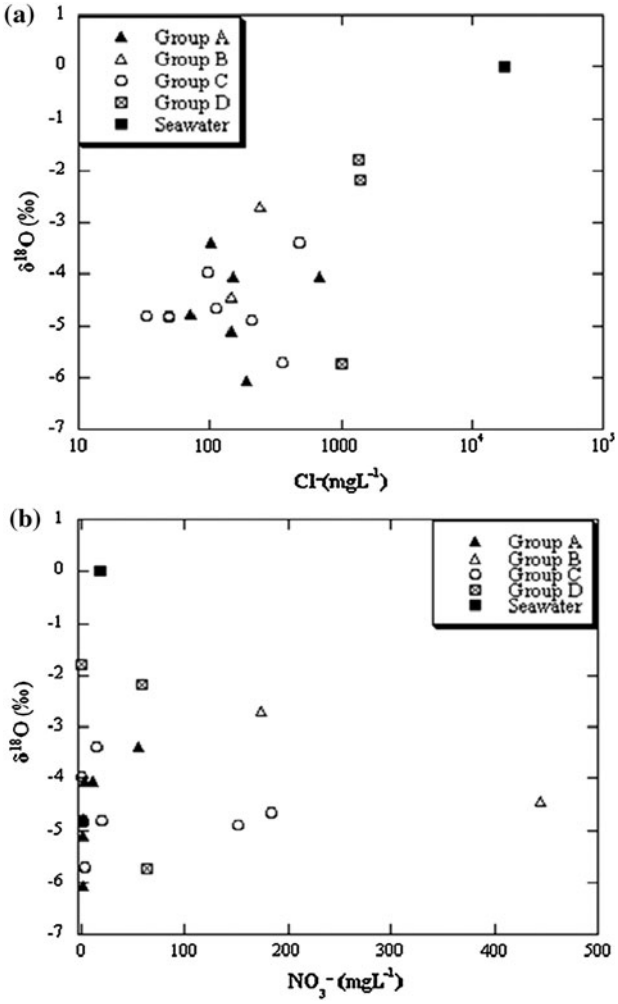

Fig. 8 Variation of $\delta^{18}O$ (‰) versus chloride concentrations (**a**), and $\delta^{18}O$ (‰) versus nitrate concentrations (**b**) of groundwater samples in the study area. Samples are sorted according to clustered groups

(Fig. 8b). The high-δ^{18}O values and salinity might reflect both evaporation/salinization processes and/or groundwater contamination from anthropogenic sources. Evaporation/salinization as the main process can be ruled out since there are no correlations between nitrate and any of the main contributors to groundwater salinity such as Cl^- (Table 3). The observed increasing concentrations of nitrate relative to δ^{18}O values, without corresponding chloride concentrations for group B samples (Fig. 8), strengthened our claim that these wells have been contaminated by anthropogenic sources. Since there are no agricultural activities around these wells, the potential sources of nitrate pollution in the area are likely to be linked to nitrate-rich water from domestic sewage. This anthropogenic recharge component represents degradation of the water quality of the aquifer, not only due to the high nitrate but also due to fecal bacteria that are commonly associated with this source.

In summary, we conclude that the high-ionic strength of water in the group B samples is derived from sewage, and groundwater salinization of groups C and D is due to seawater intrusion. The isotopic variations of group A samples did not show a significant relationship to either Cl^-or NO_3^- (Fig. 8). This groundwater is, therefore, considered to be freshwater with low concentrations of both Cl^- and NO_3^- (Table 1), and classified as a $NaHCO_3$ type of water induced mainly by dissolution of carbonate minerals and ion exchange reactions.

Conclusion

This study delineates different geochemical processes controlling the groundwater chemistry of the coastal aquifer in Tanzania. These processes are revealed by a conceptual assessment of multivariate statistical analyses on chemical tracers and stable isotopes. There are three main factors that govern the spatial variation in groundwater composition. Together, they explain 80.6% of the total variance in the groundwater quality. The first factor has high-positive loadings for most of the physicochemical parameters, and it is a representative of the degree of seawater intrusion. The second factor has high-negative loadings for pH and HCO_3^-, and a high-positive loading for DO. These points to a residence time gradient with dilution of groundwater by fresh recharge on the one extreme, and enhanced mineralization by water–soil/rock interaction on the other. The third factor has a high-positive loading for NO_3^- and K^+, and moderate loadings for Mn^{2+}. These ions are mainly associated with sewage.

HCA sorted the water samples into four groups distinguishable mainly by salinity, bicarbonate content, and nitrate concentrations. Group A is old groundwater with moderate salinity. Group B is sewage-contaminated water. Group C is freshwater–seawater mixing, with low and intermediate-salinity, and group D comprises saline intrusion water, with a high-salinity content.

The slope of the fitting line describing the δ^2H–δ^{18}O relationship for the rainwater data is typical for areas having seasonal rain and dry periods under hot climatic conditions. The stable isotope data in the shallow groundwater indicate that it is recharged by fresh precipitation and infiltration by surface water. The narrow range of depleted stable isotope values in the deep groundwater indicates that this water is old and probably derived from infiltration in the recharge zone followed by slow lateral percolation. This is also supported by the general chemical signature of deep ground water. The most important geochemical processes occurring in the studied coastal aquifer system are intrusion of seawater accompanied by cation exchange reactions, and the dissolution of carbonate minerals. The enriched δ^{18}O corresponding with high-Cl^- concentration and the strong correlation between all major ions, except NO_3^- and K^+, infer that the high-salinity in the shallow groundwater samples (group D) are due to seawater intrusion. It is also clear that the high-nitrate concentrations (up to 445 mg L^{-1}) and high-δ^{18}O values for groundwater samples in group B is due to sewage originating from the squatter settlements in Dar es Salaam.

This study shows that conceptual reasoning supported by results from multivariate statistical analysis (using HCA and FA) of chemical composition is a powerful tool for the classification of groundwater and the identification of major factors governing groundwater quality. The application of HCA techniques may be used to roughly distinguish between samples whose chemistry is governed by different mechanisms. A conceptual understanding of the role of the parameter with the strongest loadings in the FA revealed that the main governing geochemical processes included salinization, natural mineralization and anthropogenic contamination. The sample scores in the FA allow us to ascertain the predominant processes governing sample clusters from the HCA. Stable isotopes signatures compliment this assessment by suggesting groundwater origin and which pressures might be influencing the quality of the groundwater aquifer. Explicitly, the results of this study provided a conceptual understanding of groundwater characteristics in the alluvial plain of coastal area in Dar es Salaam, Tanzania, which is required knowledge for being able to make decisions toward establishing a cost-efficient and sustainable management system for this valuable freshwater resource. The best water quality was found in the lower confined aquifer. The results from this study highlight the importance of having stringent measures and a system for close monitoring in place when this aquifer is opened up for exploitation, to avoid further saltwater intrusion.

Acknowledgments This research was financially supported by the Quota Scheme Programme and the Department of Geosciences, University of Oslo. We thank the local owners of the private wells and the Dar es Salaam Water Supply Authority (DAWASA) Manager for granting us access to the wells. The authors are extremely grateful to Mr. Addo Ndimbo (Ardhi University-Dar es Salaam, Tanzania) for his support during the sampling phase of this work. We are also indebted to technicians in the Department of Geosciences laboratory, University of Oslo, for their efficient assistance in the analysis of water samples. The authors are extremely grateful to Prof. Hans Martin Seip (Department of Chemistry, University of Oslo) for earlier comments, which are greatly appreciated. The constructive comments from the journal editors and anonymous reviewers followed by the language-review done by Ms. Amy Dale from GeoResearch Consulting, Skarnes, Norway, improved the quality of the manuscript.

References

Adams S, Titus R, Pietesen K, Tredoux G, Harris C (2001) Hydrochemical characteristic of aquifers near Sutherland in the Western Karoo, South Africa. J Hydrol 241:91–103

Andreasen DC, Fleck WB (1997) Use of bromide: chloride ratios to differentiate potential sources of chloride in a shallow, unconfined aquifer affected by brackish-water intrusion. Hydrogeol J 5:17–26

Appelo CAJ (1996) Multicomponent ion exchange and chromatography in natural systems. Rev Mineral 34:193–227

Appelo CAJ, Postma D (1993) Geochemistry, groundwater and pollution. Balkema, Rotterdam, p 519

Appelo CAJ, Postman D (2005) Geochemistry, groundwater and pollution, 2nd edn. Balkema, Rotterdam, p 459

Burnett WC, Aggarwal PK, Aureli A et al (2006) Quantifying submarine groundwater discharge in the coastal zone via multiple methods. Sci Total Environ 367:498–543

Ceron JC, Jimenez-Espinosa R, Pulido-Bosch A (2000) Numerical analysis of hydrogeochemical data: a case study (Alto Guadalentõan, southeast Spain). Appl Geochem 15:1053–1067

Clark ID, Fritz P (1997) Environmental isotopes in hydrogeology. CRC, Boca Raton

Cook P, Herczeg AL (2000) Environmental tracers in subsystem hydrology. Kluwer Academic Publishers, New York

Craig H (1961) Isotopic variation in meteoric waters. Sci 133:1702–1703

Dansgaard W (1964) Stable isotope in precipitation. Tellus 16(4):436–468

Faure G, Mensing TM (2005) Isotopes: principles and applications, 3rd edn. Wiley, USA, pp 691–743

Gondwe E (1991) Saline water intrusion in southeast Tanzania. Geoexploration 27(1–2):25–34

Hach (1992) Digital titrator model 16900–01 manual. Hach Company, Loveland

Helina B, Pardo R, Vega M, Barrado E, Fernandez JM, Fernandez L (2000) Temporal evolution of groundwater composition in an alluvial aquifer (Pisuerga River, Spain) by principal component analysis. Water Res 34:807–816

JICA Report (2005) The study on water supply improvement in Coast Region and Dar es Salaam peri-urban in the United Republic of Tanzania-final report. Japan International Cooperation Agency (JICA), Dar es Salaam, Tanzania

Johnston RH (1983) The saltwater–freshwater interface in the Tertiary limestone aquifer, southeast Atlantic outer-continental shelf of the USA. J Hydrol 61:239–249

Kent PE, Hunt JA, Johnstone DW (1971) The geology and geophysics of coastal Tanzania. Geophysical paper 6. Her Majesty's Stationary Office (HMSO), London, pp 20–25

Kharaka YK, Carothers WW (1986) Oxygen and hydrogen isotope geochemistry of deep basin brines. In: Fritz P, Fontes JC (eds) Handbook of environmental isotope geochemistry, vol 2. Elsevier, Amsterdam, pp 305–361

Kim Y, Lee KS, Koh DC, Lee DH, Lee SG, Park WB, Koh GW, Woo NC (2003) Hydrogeochemical and isotopic evidence of groundwater salinization in a coastal aquifer: a case study in Jeju volcanic island, Korea. J Hydrol 270:282–294

Kim JH, Kim RH, Lee J, Cheong TJ, Yum BW, Chang HW (2005a) Multivariate statistical analysis to identify the major factors governing groundwater quality in the coastal area of Kimje, South Korea. Hydrol Process 19:1261–1276

Kim JH, Lee J, Cheong TJ, Kim RH, Koh DC, Ryu JS, Chang HW (2005b) Use of time series analysis for the identification of tidal effect on groundwater in the coastal area of Kimje, Korea. J Hydrol 300:188–198

Lee JY, Cheon JY, Lee KK, Lee SY, Lee MH (2001) Statistical evaluation of geochemical parameter distribution in a ground water system contaminated with petroleum hydrocarbons. J Environ Quality 30:1548–1563

Liu CW, Lin KH, Kuo YM (2003) Application of factor analysis in the assessment of groundwater quality in a blackfoot disease area in Taiwan. Sci Total Environ 313:77–89

Ministry of Water (2006) MAJI review (Draft). The United Republic of Tanzania, Dar es Salaam

Morell I, Gimenez E, Esteller MV (1996) Application of principal components analysis to the study of salinization on the Castellon Plain Spain. Sci Total Environ 177:161–171

Nicholson SE (1996) A review of climate dynamics and climate variability in Eastern Africa. In: Johnson TC, Odada EC (eds) The limnology, climatology and paleoclimatology of the East African Lakes. Gordon and Breach, Amsterdam, pp 25–56

Nkotagu H (1989) Geochemistry of shallow groundwater at Kigamboni peninsula along Dar es Salaam coastalstrip Tanzania. J Afican Earth Sci 9(3–4):739–748

Nkotagu H (1996) Application of environmental isotopes to groundwater recharge studies in a semi-arid fractured crystalline basement area of Dodoma, Tanzania. J African Earth Sci 22(4):443–457

Norwegian Consultancy (NORCONSULT) (2008) Development of a future water source for Dar es Salaam. supervision status report: Sites Kimbiji, Mpiji and Mpera. Ruden Aquifer Development Ltd, N-1628 Engelsviken, Norway for NIVA/NORCONSULT

Ozler HM (2003) Hydrochemistry and salt–water intrusion in the Van aquifer, east Turkey. Environ Geol 43:759–775

Parkhurst DL, Appelo CAJ (1999) User's guide to PHREEQC (version 2)—a computer program for speciation, reaction-path, advective-transport, and inverse geochemical calculations: US Geological Survey—Water Resources Investigations report. US Geological Survey, Denver, pp 99–4259

Richter BC, Kreitler CW (1993) Geochemical techniques for identifying sources of ground-water salinization. CRC Press, Boca Raton, p 258

Rietti-Shati M, Yam R, Karlen W, Shemesh A (2000) Stable isotope composition of tropical high-altitude fresh-waters on Mt. Kenya, Equatorial East Africa. Chem Geol 166:341–350

Ruden F (2007) The discovery of a regional Neogene aquifer in coastal Tanzania. Coastal aquifers: challenges and solutions 1. Instituto Geológicoy Minerode España, Madrid, pp 363–372

Stigter TY, Carvalho Dill AMM, Ribeiro L, Reis E (2006) Impact of the shift from groundwater to surface water irrigation on aquifer dynamic and hydrochemistry in a semi-arid region in the south of Portugal. Agric Water Manag 85(1–2):121–132

Stoessell RK (1997) Delineating the chemical composition of the salinity source for the saline groundwaters: an example from East-Central Concordia Parish, Louisiana. Ground Water 35: 409–417

Suk H, Lee KK (1999) Characterization of a ground water hydrochemical system through multivariate analysis: clustering into ground water zones. Ground Water 37:358–366

Thyne G, Guler C, Poeter E (2004) Sequential analysis of hydrochemical data for watershed characterization. Ground Water 42:711–723

Tijani MN (2004) Evolution of saline waters and brines in the Benue-Trough, Nigeria. Appl Geochem 19:1355–1365

TPDC (2007) http://www.tpdc-tz.com/new/table2.htm. Accessed 15 December 2007

Vogt et al (2001) IMPACTS catchment manual. http://www.iis.niva.no/IMPACTS/. Accessed 17 Feb 2009

WHO (2004) Guidelines for drinking-water quality, 3rd edn, vol 1. Recommendations. World Health Organization, Geneva

Word JH (1963) Hierarchical grouping to optimize an objective function. J Am Stat Assoc 58:236–244